



## Towards a better knowledge of the clastic Lower Triassic reservoirs in the Upper Rhine Graben (France)

Chrystel Dezayes, Isabelle Thinon, Gabriel Courrioux, Sébastien Haffen,  
Vincent Bouchot

### ► To cite this version:

Chrystel Dezayes, Isabelle Thinon, Gabriel Courrioux, Sébastien Haffen, Vincent Bouchot. Towards a better knowledge of the clastic Lower Triassic reservoirs in the Upper Rhine Graben (France). World Geothermal Congress 2010, Apr 2010, Bali, Indonesia. 7 p. hal-00491078

**HAL Id: hal-00491078**

**<https://hal-brgm.archives-ouvertes.fr/hal-00491078>**

Submitted on 10 Jun 2010

**HAL** is a multi-disciplinary open access archive for the deposit and dissemination of scientific research documents, whether they are published or not. The documents may come from teaching and research institutions in France or abroad, or from public or private research centers.

L'archive ouverte pluridisciplinaire **HAL**, est destinée au dépôt et à la diffusion de documents scientifiques de niveau recherche, publiés ou non, émanant des établissements d'enseignement et de recherche français ou étrangers, des laboratoires publics ou privés.

## Towards a better knowledge of the clastic Lower Triassic reservoirs in the Upper Rhine Graben (France)

Chrystel Dezayes\*, I. Thinon\*, G. Courrioux\* S. Haffen\*\*, V. Bouchot\*

\* BRGM (French Geological Survey), BP36009, F-45060 Orléans Cedex. \*\* Université de Strasbourg, F-67084 Strasbourg.

c.dezayes@brgm.fr

**Keywords:** Geothermal potential, Rhine Graben, Clastic reservoir, Trias.

### ABSTRACT

To develop the sustainable energy in France, we propose a methodology for estimation of the geothermal potential in a limited area. This method is applied to the Upper Rhine Graben, for the resource located in clastic formation of the lower Triassic unit, namely the Buntsandstein. The methodology is based on Muffler & Cataldi works (1978) and the computation of the heat in place and exploitable heat.

A 30km x 35km area located between Strasbourg and Obernai in France has been investigated. Based on a detailed geological study combining data derived from 13 previous oil boreholes and 143km length of seismic profiles, the main sedimentary interfaces including geological layers and faults have been interpreted between the outcropping Quaternary layers and the deeper parts made of Permo-Triassic formations. From that interpretation, 3D geological models have been yielded based on different hypotheses. These models, constructed with the GeoModeller software developed by BRGM, allow calculating the volume of modelled silicoclastic formations. According to the modelling results, different reservoir volumes have been computed which impacts the estimation of the overall geothermal potential. Temperature conditions derived from BHT (Bottom Hole Temperature) data in boreholes reaching the Buntsandstein sandstones, show a high average geothermal gradient (between 50°C/km and 58°C/km), which tends to indicate a significant geothermal potential. In the investigated area, the volume of the Buntsandstein reservoir is about 300km<sup>3</sup> and the exploitable heat quantity is around 350 GW<sub>th</sub>.year ± 5%.

For the future, we start a characterization of the Buntsandstein formation in terms of petrophysics to better assess the quality of the geothermal resource and to define exploitation target.

### 1. INTRODUCTION

In France, the geothermal heating production is mainly concentrated within the Paris Basin, where about 30 geothermal doublets have been exploiting the Dogger limestone reservoir since the 80's. They produce about 4000 TJ.year with an installed capacity of about 240MWt (Laplaige *et al.*, 2005). The development of renewable energy necessitates exploring new or poorly well-known deeper sedimentary geothermal reservoirs, located in other promising areas. In this framework, we conducted a study about the deep sedimentary geothermal potential of the Rhine graben for heat and/or electricity production (Dezayes *et al.*, 2007; Dezayes *et al.*, 2008). The geothermal resource belongs to the silico-clastic formations embedded within the thicker (about 400m) Triassic

sediments made of argillaceous sandstones. Temperatures are often higher than 100°C based on previous deep geothermal borehole data (Cronenbourg, Rittershoffen, Soultz; Munck *et al.*, 1979).

The goal of this study is to set up a whole methodology for estimating the geothermal potential of the studied area. This assessment is based on the definition of the part of accessible resource "that could reasonably be extract at costs competitive with other forms of energy at some specified future time" (Muffler & Cataldi, 1978). To quantify this resource, we calculate the quantity of heat, which could be extracted from a rock volume (1):

$$Q = \rho.C_p.V.(T_i - T_f) \quad (1)$$

where  $\rho$ ,  $C_p$ ,  $V$ ,  $T_i$ ,  $T_f$  are rock density, heat capacity, volume of rock, initial temperature of the reservoir and final temperature after the total exploitation of the reservoir, or surface temperature, respectively.  $Q$  represents the heat extracted in Joule when the temperature decreases from  $T_i$  to  $T_f$ .

The volume of the reservoir is one parameter, which is not easy to estimate in a graben context because of intense faulting. This paper presents a 3D geometrical model of the Buntsandstein formation in a limited area of the Rhine graben located near to Strasbourg, where the population density is high. This model is based on an analysis of borehole data and reflexion seismic profiles. Moreover, we start a characterisation of the reservoir quality of the Buntsandstein to better qualify the geothermal resource of this formation.

### 2. LOCAL GEOLOGY

The Rhine Graben is located in the extreme NE part of France with its western part and in Germany for its eastern part. The graben is 30-40km large and 300km long and the Rhine river flows through it (Figure 1).

This graben belongs to the Cenozoic peri-alpine rifts namely the West European Rift System (Ziegler, 1992), which is well-known because of numerous petroleum and mining exploration campaigns (boreholes, geophysical surveys...). The filling is composed by Tertiary and Quaternary sediments with a rather discrete volcanic activity, which overlays the Jurassic and Triassic sediments and the Paleozoic crystalline basement.

This graben is formed by three segments limited by border faults oriented N15°E in the North and the South parts, and N30-35°E in the middle part (Figure 1). Two crystalline massifs surround it with the Vosges massif on the western part and the Black Forest on the eastern part. Between these mountains and the Rhine valley are located fracture fields. They are bands of fractured terrains, which collapse

progressively giving a general framework in stairs (Figure 1). In the North, the rift valley is limited by the Hercynian fault of the Rhenish Shield and in the South, by the Jura front and the transfer Rhine/Saône fault. This fault allows the link with other Tertiary grabens, namely the Bresse and the Limagne grabens (Bergerat and Geyssant, 1980).

Several major subsidence phases related to the Rhine graben tectonics generated variable sediment thicknesses. The subsidence starts at the end of Eocene (Lutetian) and continues during Oligocene with an E-W extensional regime. From the Upper Oligocene (Chattian), the subsidence is different between the northern and the southern parts of the graben, on both sides of the Erstein limit, which is the continuation of the regional Lalaye-Lubine-Baden-Baden hercynian fault (Villemin *et al.*, 1986; Schumacher, 2002). In the southern part, the subsidence decreases and stops at the end of Oligocene (Chattian-Aquitanian). By the end of the subsidence, the graben borders raises inducing the uplift of the Vosges and the Black Forest massif. In the northern part of the graben, the subsidence is quite regular and homogenous until the Upper Miocene. The subsidence rate is less important and the graben borders are less uplifted (Villemin *et al.*, 1986).

Due to the rifting, Moho uplifts implying a large-scale geothermal anomaly (Dezès and Ziegler, 2001). Associated to that, small scale geothermal anomalies are due to fluid circulations within fracture zones (Figure 1; Pribnow and Schellschmidt, 2000). These local anomalies are mainly located along the Western border of the graben and the fluid circulates from East to West associated with the border faults (Benderitter and Elsass, 1995; Pribnow and Clauser, 2000). Inside the Rhine graben, several local thermal anomalies occurred and are spatially distributed from the South to the North: Selestat, Strasbourg, Soultz (in superimposition with the petroleum field of Pechelbronn), Landau (also a petroleum field), Wattenheim (NE Worms) and Stockstadt (SW Darmstadt) (Figure 1).

The studied area corresponds to the anomaly located close to Strasbourg and Obernai, in the South-West part of the town (Figure 1). The dimension is about 30kmX35km and is located on the West border of the graben, near the Rhenane fault and at the South point of the Saverne fracture field (Figure 1). At the graben scale, the temperature extrapolated at 1500m indicates 100°C that shows a thermal gradient of 66°C/km (Figure 1).

In this zone, a detailed study has been done from borehole data and seismic profiles in order to outline the geometry of the clastic reservoir of the Buntsandstein sandstones and to determine its geothermal characteristics (temperature, flow

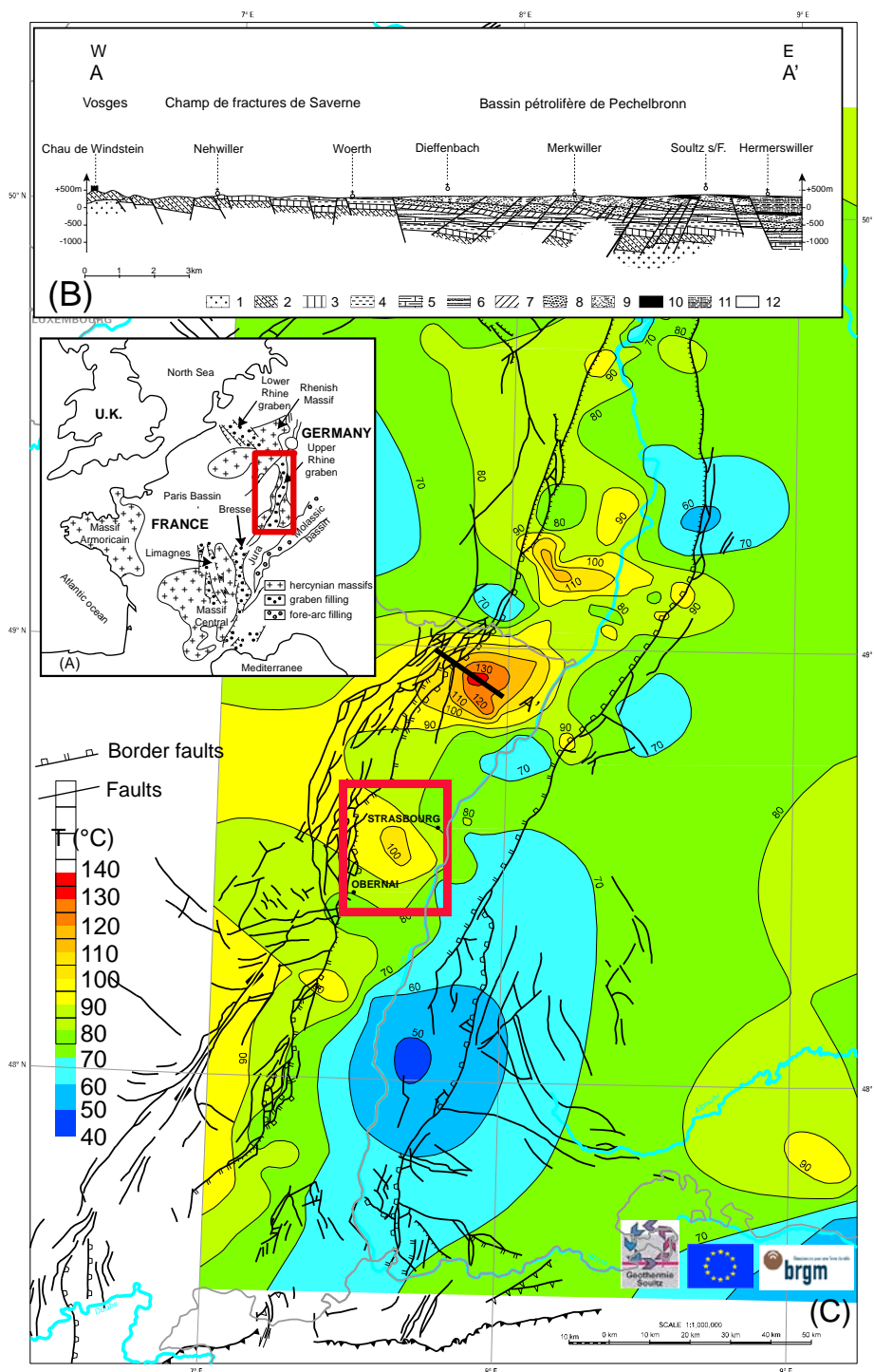


**Figure 1: Geological setting of the Upper Rhine Graben.**  
**A- Location of the Upper Rhine Graben within the West European Rift System. B- Cross-section of the western part of the Rhine Graben (Sittler, 1985). C- Structural map of the Upper Rhine Graben and temperature distribution extrapolated at 1500m depth (GGA Hannover database in Genter *et al.*, 2004). Red square: location of the local study.**

rate, thickness, depths, ...). From these data and the petrophysical properties of this aquifer, an estimation of the geothermal potential of this limited area has been evaluated.

### 3. DATA AVAILABLE

Oil exploration was extensive in the Upper Rhine Graben. A lot of seismic profiles have been acquired in the framework of the petroleum exploration between the 70's and 80's. A selection of 143km of seismic reflection profiles, collecting data from previous surveys of 1975, 1985 and 1987, has been reprocessed (the velocity analysis have been improved) and reinterpreted in order to determine the geometry of the main interfaces of the geological formations embedded the geothermal sandstone reservoirs (Figure 2). Five seismic cross sections are transverse to the graben structures and two others are oriented parallel to the graben axis that means they cross cut the first ones (Figure 2). At the extreme southern part of the investigated area, the transverse seismic line 87ADL1, is not crossed by any of the longitudinal seismic lines, that will poorly constrain the geological interpretation.

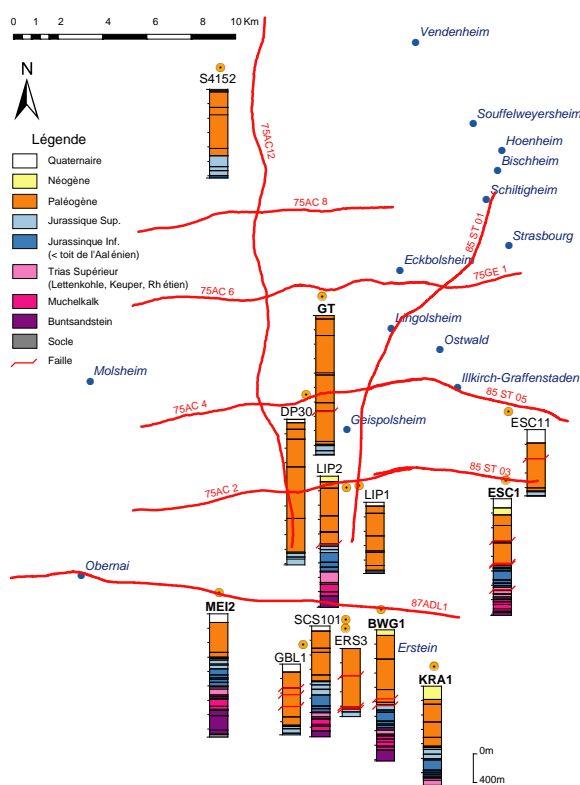


**Figure 2: Location of boreholes and seismic profiles, and geological logs in the boreholes. Boreholes with bold name have well velocity surveys.**

In order to convert the time of the seismic interpretations in depth, we use the velocity fields measured in the boreholes to calibrate the seismic horizons of the seismic lines with the geological formations of the boreholes. Only five well velocity surveys exist but the borehole repartition is heterogeneous: four of them (MEI2, BWG1, KRA1, ESC1) reach the Triassic formations and give velocity field for the whole sedimentary cover. Unfortunately, they are concentrated in the southern and eastern boundary of the studied zone (Figure 2). The other borehole (GT), located in the centre of the studied area, reaches only the top of Jurassic.

The velocity field on the whole studied zone is poorly constrained considering the structural complexity of the

studied zone. However, the seismic lines have been interpreted to determine the location of faults and the limits of main formations such as the top of Pechelbronn layers, the base of Tertiary, the top of Aalenian, the top of Trias, the top of Muschelkalk, the top of Buntsandstein and the top of crystalline basement (Figure 3).

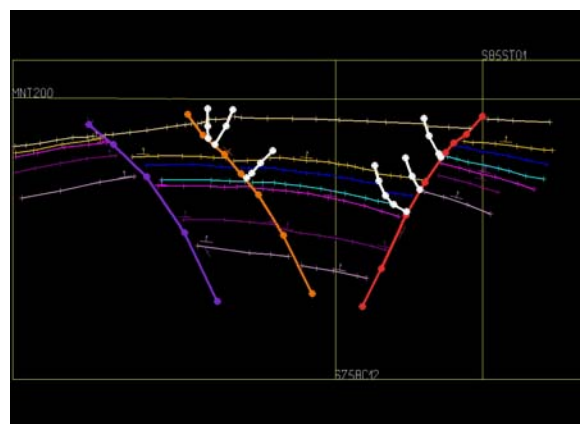


**Figure 3: Example of interpreted seismic cross-section (75AC2 profile) (total cross-section length: 12.5km).**

Other boreholes complete the study (Figure 2). They reach at least the Jurassic formations, where the Grande Oolithe is an aquifer reservoir, and 5 of them reach the Triassic sandstone (Figure 2). The Meistratzheim-2 (MEI2) borehole reaches the crystalline basement and constitutes a good reference borehole for defining lithology.

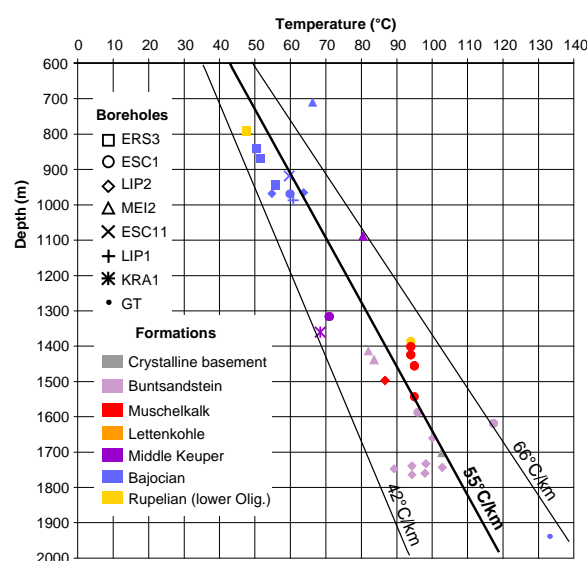


**Figure 4: Temperatures in the previous oil boreholes and calculated geothermal gradient. Location of boreholes: Figure 2.**

As there are boreholes for petroleum exploration, only Bottom Hole Temperature (BHT) is available. These BHT data are measured in almost all industrial wells at the deepest part of the well immediately after the end of drilling phase and are then thermally disturbed by the mud circulation. The raw data have been corrected by statistical method (AAPG; Bodner et Sharp, 1988) or analytical method (ICS; Goutorbe *et al.*, 2007). Then, these temperatures indicate a geothermal gradient ranging between 42°C/km and 66°C/km, with an average at 52°C/km (Figure 4).

This thermal gradient deduced from borehole data is twice those well known in the Paris Basin. The curve of the temperature vs depth shows regular evolution with depth and is not influenced by the lithology (Figure 4).

The normal faults are NNE-SSW striking and dipping eastward or westward forming horst-graben and half-graben structures. Inside the faulted compartments, the sedimentary layers show tilted blocks with opposite tilting.

#### 4. 3D MODEL BUILDING

Thanks to the GeoModeller software developed by BRGM, a 3D model of the deep Triassic sandstone formation is outlined. The modeled area is a 30km on X-axis (E-W), 32km on Y-axis (N-S) and 7km along the vertical. In this software, faults are explicitly represented by limited or unlimited surfaces whereas the litho-stratigraphic interfaces are interpolated (Figure 5), using potential field cokriging method (Lajaunie *et al.*, 1997). In this method, one takes simultaneously into account interface locations, orientation data and fault influence.

In the northern part of the area, where the 6 seismic lines are intersecting each others forming a grid pattern, the fault correlations are well constrained, forming horst and graben structures or half-grabens. However, the southern cross-section, namely the 87ADL1 seismic profile, shows another fault pattern, with a large graben in the West part and a series of numerous dipping eastward faults in the eastern part.

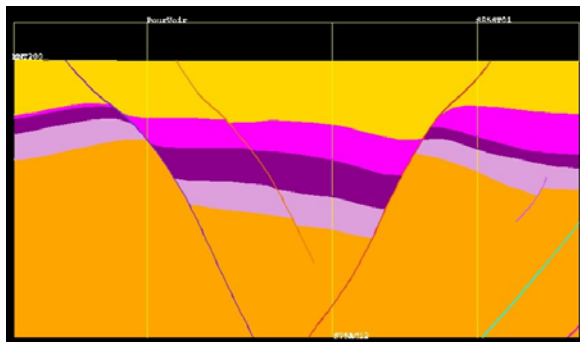


**Figure 5: Example of interpolated interfaces and faults in a seismic cross-section (75AC2 profile). Yellow: Tertiary, pink: Jurassic and upper? Trias, purple: Muschelkalk, violet: Buntsandstein, orange: granitic basement (total cross-section length: 12.5km).**

The difference between structural pattern in the northern part and in the southern part of our studied could be explained by the Southern Transfer Zone of the Rhine Graben. At the graben scale, this transfer zone subdivides the graben into a northern and a southern half-graben with opposite polarities and master fault shifts from the eastern to the western margin (Derer *et al.*, 2005). In the basement, this transfer zone is associated to the WSW-ENE-strike-slip Variscan Lalaye-Lubine-Baden-Baden fault zone (Villemin *et al.*, 1986; Schumacher, 2002).

As our studied zone is located in the vicinity of this transfer zone, the tectonic evolution appears complex. Fault trace correlation is then complicated by the presence of this transfer zone. Different configurations of linking fault traces are tested, according to their location, apparent slip throw and dip direction. We look at the effect of each configuration on interface interpolations. This leads us to retain hypothesis which leads to the minimum intra-block

distortion in the interfaces. As an example, the configuration shown on Model A is not really satisfactory because it shows a large distortion on a fault in the SW part of the model (Figure 6).

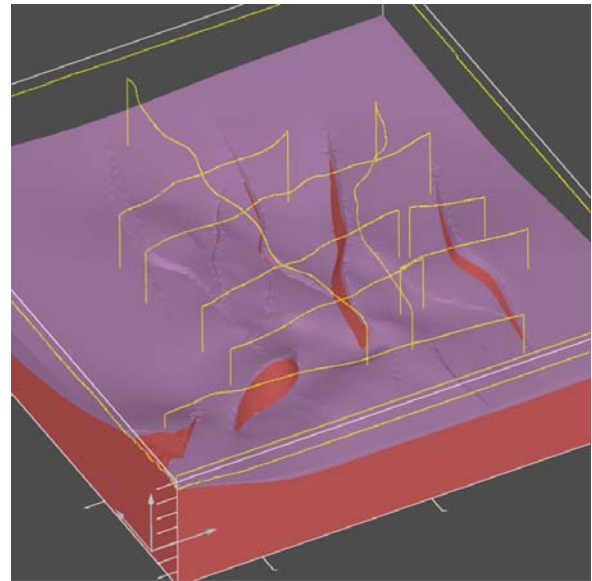


**Figure 6: View to the NE of the model A, which is not satisfactory because of intra-block distortion. Violet Buntsandstein reservoir, red: crystalline basement (30km on E-W axis and 32km on N-S axis).**

The Model B is more acceptable because the throws of the faults are homogeneous (Figure 7). However, we have kept the both models to compare the geometry of the reservoir with the geothermal potential computation.

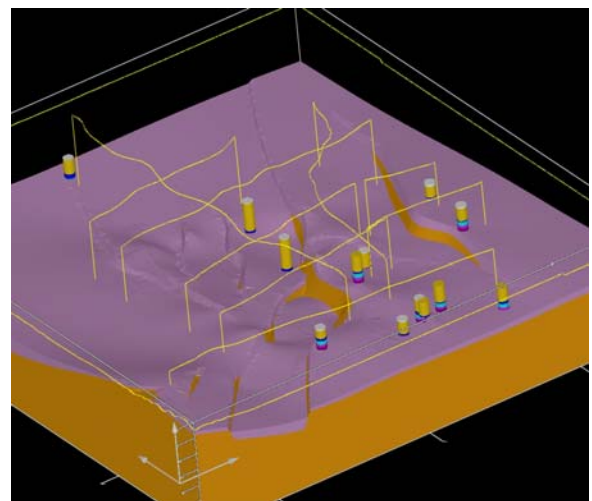


**Figure 7: View to the NE of the acceptable model B. Violet: Buntsandstein reservoir, orange: crystalline basement. The cylinders represent the boreholes (30km on E-W axis and 32km on N-S axis).**

This most probable geological model shows a fault network with NNE-SSW striking orientation (Figure 7). In the southern part of the model, the basement is at around 2000m depth, whereas in the northern part, the basement ranges between 3400m and 4000m depth.



A huge fault crosses the model area and has a dip-slip throw higher than 1000m. This fault is associated in the SE part of the model with another huge fault with a throw of around 1000m, forming a graben structure with NE-SW striking orientation. In the deeper part of this graben, the basement is at 3800m depth (Figure 7).

It appears that the building of the fracture network is not easy. In our case, other seismic profiles exist between that interpreted here. These other seismic profiles could help us to constrain our model.

## 5. RESERVOIR GEOMETRY

Based on the both 3D model (Model A and Model B), 2D thickness maps have been exported with a 200m grid resolution (Figure 8 and Figure 9).

The top of the Buntsandstein sandstones indicates a general deepening to the North. In the northern part of the studied area, the top of the Buntsandstein ranges between 3200m and 3700m depth, and reaches 3880m depth at the base of the central tilted block. In the southern part, the top of the Buntsandstein reaches 1000m to 1500m depth and 200-300m depth in the border of the Vosges massif. Between the faults, the major tilted blocks are dipped to the East.

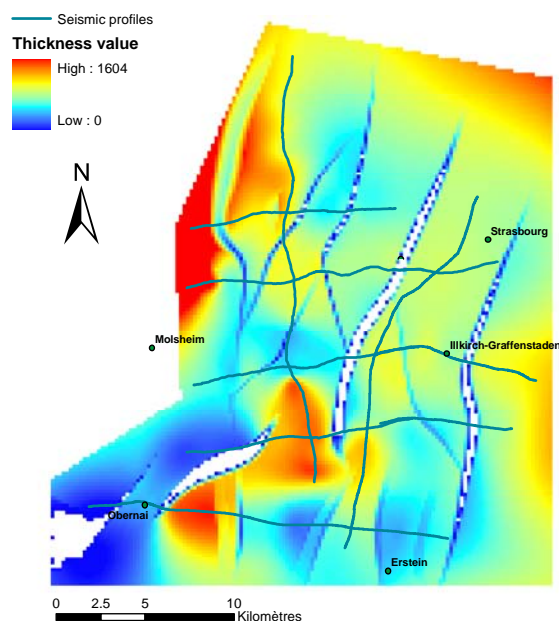


**Figure 8: Thickness map of the top of Buntsandstein with a 200m mesh for Model A (see Figure 6).**

The thickness map permits to compute the volume of the formation reservoir in the studied area to estimate the geothermal potential of the reservoir. For the Model A (Figure 8), the volume of the Buntsandstein formation including the Permian Rotliegende sandstones reaches is 275km<sup>3</sup>. In this case with the Model B (Figure 9), this volume is around 302km<sup>3</sup>.

The thickness of the Buntsandstein reservoir is in average between 300m and 500m (Figure 8 and Figure 9). At the centre of sub-basin and in the western border, the thickness reaches 1000m. However, it seems that the identified formation includes the Permian sandstones of Rotliegende and could not be distinguished easily with seismic profiles. These Rotliegende sediments are not continuous in the whole Rhine graben, but occur mainly in the North and in the graben center. They could reach around 500m thickness

in the graben centre (Munck *et al.*, 1979). These sandstones are gas reservoir in the northern part of Germany and could be geothermal reservoir, but they are poorly well-known in the Upper Rhine graben. They are generally interpreted as filling late-Hercynian grabens.

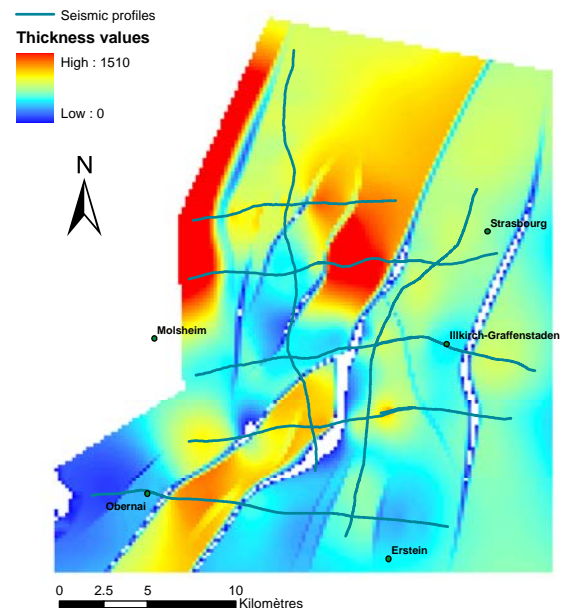


**Figure 9: Thickness map of the Buntsandstein with a 200m mesh for Model B (see Figure 7).**

## 6. GEOTHERMAL POTENTIAL

The results of borehole temperature analysis combined with the geological modeling were used to compute the heat quantity as we described previously (Eq (1)).

The parameters  $\rho$  and  $C_p$  are depending of the nature of the rock and could spatially vary. However, in this case, we take mean values for sandstone (Table 1). The average of temperature measured in the Buntsandstein formation (Figure 4) is taking into account (Table 1). The final temperature is usually taken at 10°C.

Rock density	$\rho$	2200 kg/m <sup>3</sup>
Rock heat capacity	$C_p$	710 J/kg.K
Initial temperature	$T_i$	100°C
Final temperature	$T_f$	10°C
Volume for Model A	$V$	275 km <sup>3</sup>
Volume of Model B	$V$	302 km <sup>3</sup>

**Table 1: Value of parameters taken into account of the heat quantity in the Buntsandstein sandstones.**

For the Buntsandstein reservoir within the studied area and with the Model B (Figure 7), the computation gives  $Q$  (heat in place)  $\approx 1346$  GW<sub>th</sub>.year.

If we consider the Model A (Figure 6), the reservoir volume will be 275km<sup>3</sup> and the heat removed will be 1224 GW<sub>th</sub>.year.

This quantity of the thermal energy represents the geothermal resource base ( $Q$  heat in place) and not the power that can be generated ( $Q_{\text{expl}}$  exploitable heat). The size of the accessible resource is much smaller that implied by this simplistic analysis. Only a part of this resource is extracted and defined by a recovery factor,  $R$ , that depends on the extraction technology used (Muffler & Cataldi, 1978; Hurter & Schellschmidt, 2003). This recovery factor

R is constituted by a “temperature factor” ( $R_T$ ) and a “geometric factor” ( $R_G$ ). In a doublet system, where there are a production borehole and an injection borehole, it can be shown that (Lavigne, 1978):

$$R_T = \frac{T_i - T_{inj}}{T_i - T_f} \quad (2)$$

$T_{inj}$  is the injection temperature. A group of experts of the European Commission recommended a value of 25°C for  $T_{inj}$  (Hurter & Schellschmidt, 2003).

The “geometric factor” is an empirical value (Lavigne, 1978). For an aquifer reservoir, the geometric factor is 0.33 (Hurter & Schellschmidt, 2003), then:

$$R_T = 0.33 \cdot \frac{T_i - T_{inj}}{T_i - T_f} \quad (3)$$

And then, the assessment of exploitable heat quantity is given by (4):

$$Q_{expl} = R \cdot Q \quad (4)$$

In our case, the temperature factor  $R_T = 83\%$  and the recovery factor  $R = 27.5\%$ , then the heat could be exploited is between  $Q_{expl} = 337 \text{ GW}_{th\cdot\text{year}}$  and  $Q_{expl} = 370 \text{ GW}_{th\cdot\text{year}}$  for the geological model A and B.

## 7. FEATURES OF THE BUNTSANDSTEIN RESERVOIR

To better characterize the geothermal reservoir of the Buntsandstein in the Rhine Graben, we have started a new scientific project with collaboration with the University of Strasbourg. This project aims to characterize parameters of the Buntsandstein reservoir in terms of petrophysics, diagenesis, fracture network, inside the Rhine graben based on borehole cores and outcrops on both sides of the Rhine graben.

First, we would like to underline if the Buntsandstein show heterogeneity of several origin (sedimentary, diagenesis, fracturation) and their incidence on the reservoir quality. Second, these new data will improve fluid flow models in the Buntsandstein for better evaluating the geothermal resource. Finally, we will be able to focus different geothermal targets in the Rhine graben to implant doublet for exploiting the geothermal resource.

## 8. CONCLUSIONS

The silico-clastic formation of Buntsandstein shows a high potential for geothermal resource in the Upper Rhine Graben. This study, made at local scale, allowed us to provide a preliminary assessment of this favourable reservoir, in a populated area.

We focused on a 30kmX35km area, in the south-western of Strasbourg, based on borehole data and seismic profiles. A 3D model of this area has been yielded to obtain the precise shape of the reservoir.

With this model, we underlined a sub-graben located in the SW part of the studied area. The northern part of the area shows a different tectonic pattern with half-grabens and tilted blocks. This difference could be explained by the Southern Transfer Zone of the Rhine Graben located in the

Erstein ridge and could be the continuity of the Lalaye-Lubine Hercynian fault (Schumacher, 2002; Derer *et al.*, 2005).

The interpretation of the geological area influences greatly the shape of the reservoir formation and its volume taken into account for the geothermal potential assessment. In our case, our interpretation implies a 300km<sup>3</sup> volume for the Buntsandstein reservoir formation. However, we can not clearly distinguish the Permian sandstones, which are not easily differentiated, from the Buntsandstein sandstones in the seismic profiles. The exploitable geothermal potential taking into account these two sandstone formations is assessed at 350 GW<sub>th</sub>·year ±20.

To improve this first assessment of the Buntsandstein, we are starting a characterisation of the geothermal reservoir quality based on petrophysics measurements, diagenesis study, etc... within the Rhine graben and on their borders.

## ACKNOWLEDGEMENTS

We are grateful to Ademe (French agency for Environment and Energy), which has financially supported this work with BRGM (CLASTIQ and CLASTIQ-2 projects). The main author thanks to Typhaine Duval and Gloria Heilbronn, two students who are contributed to the seismic interpretation and the building of the model.

## REFERENCES

- Benderitter Y., Elsass P. (1995) - Structural Control of Deep Fluid Circulation at the Soultz HDR Site, France: a Review, *Geothermal Science and Technology*, 4, p. 227-237.
- Bergerat, F. & Geyssant, J. (1980) - La fracturation tertiaire de l'Europe du Nord : résultat de la collision Afrique-Europe. *C. R. Acad. Sci. Paris* **290**(D), p. 1521-1524.
- Bodner D. P., Sharp J.M.J. (1988) – Temperature variations in South Texas subsurface. *Am. Ass. Petr. Geol. Bull.*, 72, p. 21-32.
- Derer C., Schumacher M., Schäfer A. (2005) – The northern Upper Rhine Graben: basin geometry and early syn-rift tectono-sedimentary evolution. *Int. J. Earth Sci. (Geol. Rundsch)*, 94, p.640-656.
- Dezayes C., Thion I., Courrioux G., Tourlière B., Genter A. (2007) - Estimation du potentiel géothermique des réservoirs clastiques du Trias dans le Fossé rhénan. *Final report. BRGM/RP-55729-FR*, 72 p.
- Dezayes C., Genter A., Thion I., Courrioux G., Tourlière B., (2008) – Geothermal potential assessment of clastic triassic reservoirs (Upper Rhine Graben, France). *32<sup>nd</sup> Workshop on Geothermal Reservoir Engineering*. Stanford, California, January 28-30, 2008.
- Dèzes, P. and Ziegler, P. A. (2001) - European Map of the Mohorovicic discontinuity. *2nd EUCOR-URGENT Workshop* (Upper Rhine Graben Evolution and Neotectonics), Mt. St. Odile, France.
- Genter A., Guillou-Frottier L., Breton J.P., Denis L., Dezayes Ch., Egal E., Feybesse J.L., Goyeneche O., Nicol N., Quesnel F., Quinquis J.P., Roig J.Y., Schwartz S. (2004) - Typologie des systèmes géothermiques HDR/HFR en Europe. Rapport final. BRGM/RP-53452-FR, 165 p., 75 fig., 10 tabl.

- Goutorbe B., Lucazeau F., Bonneville A. (2007) – Comparison of several BHT correction methods: a case study on an Australian data set. *Geoph. J. Int.*, V.170, issue 2, p. 913-922.
- Hurter S. & Schellschmidt R. (2003) – Atlas of geothermal resources in Europe. *Geothermics*, 32, p.779-787.
- Lajaunie C., Courrioux G. and Manuel L. (1997) - Foliation fields and 3D cartography in geology: principles of a method based on potential interpolation, *Mathematical Geology*, 29(4):571–584.
- Laplaige P., Lemale J., Decotegnie S., Desplan A., Goyeneche O., Delobelle G. (2005) – Geothermal resources in France. Current situation and prospects. Proceedings World Geothermal Congress 2005, Antalya, Turkey, 24-29 April 2005.
- Lavigne J. (1978) – Les ressources géothermiques françaises. Possibilités de mise en valeur. *Ann. Des Mines*, April, p.1-16.
- Muffler P. & Cataldi R. (1978) – Methods for regional assessment of geothermal resources. *Geothermics*, 7, p.53-89.
- Munck F., Walgenwitz F., Maget P., Sauer K., Tietze R. (1979) – Synthèse géothermique du Fossé rhénan Supérieur. *Commission of the European Communities. BRGM Service Géologique Régional d'Alsace – Geologisches Landesamt Baden-Württemberg.*
- Pribnow D., Clauser C. (2000) - Heat- and fluid-flow at the Soultz hot-dry-rock system in the Rhine Graben. *In: World Geothermal Congress, Kyushu-Tohoku, Japan*, p. 3835-3840.
- Pribnow D., Schellschmidt R. (2000) - Thermal tracking of upper crustal fluid flow in the Rhine Graben. *Geophysical Research Letters*, 27(13), p. 1957-1960.
- Schumacher, M. (2002) – Role of pre-existing structures during rift evolution. *Tectonics*, vol. 21, n°1.
- Sittler (1985) – Les hydrocarbures d'Alsace dans le contexte historique et géodynamique du Fossé rhénan. The case history of oil occurrence in the Rhine rift valley of Alsace. *Bull. Centres Rech. Explr.-Prod. Elf-Aquitaine*, vol. 9, n°2, 253-699.
- Villemin T., Alvarez F., Angelier J. (1986) - The Rhinegraben: extension, subsidence and shoulder uplift. *Tectonophysics*, 128, p. 47-59.
- Ziegler P. (1992) – European Cenozoic rift system. *Tectonophysics*, 2008, p.91-111.